Maximum Power Point Tracking System in Photovoltaic Panels with Thermoelectric Energy Conversion

Ivo André Vieira Cleto, Instituto Superior Técnico

Abstract

This work appears in the current context of the growth in the demand of energy from renewable sources. An hybrid photovoltaic system, PV-TEG, is studied and designed, which combines photovoltaic panels (PV) and thermoelectric generators (TEG) together. This solution was designed so that the overall efficiency of solar energy conversion (partly luminous, partly thermal) could be increased, since in photovoltaic systems it is not usual to recover the energy lost through heat. Thus, the possibility of increasing the efficiency of the system is offered, making this energy more convenient to be used. Calculations and sizing are made for the filters of the converters present in the system, as well as the photovoltaic panel and the thermoelectric modules. There is also an MPPT algorithm based on the incremental conductance method that allows the panel to always present the maximum output power under the conditions present at a given moment. In order for the system to be able to interconnect the grid, it is necessary to guarantee the quality of the energy to be injected into it, with a control of the output voltage and current, carried out in the inverter downstream of the system. Finally, simulations are carried out, results are analyzed and the feasibility of the system in real context is discussed.

1. Introduction

1.1. Motivation

Since the beginning of Humanity's existence, obtaining, using and recently storing energy has been fundamental for human development, with the heat energy of fire being the primordial form of discovered energy, which allowed an unprecedented development. The Industrial Revolution (mid-eighteenth to mid-nineteenth century) brought a new approach to daily life, which then became much more dependent on energy use.

Since then, there has been an increase in the consumption of fossil fuels, which has caused the levels of greenhouse gases worldwide to escalate to an extremely dangerous level, not only for the planet but also for the human being. It was in this perspective that the Paris Agreement (2015) was drawn up, which aims to contain global warming below 2 °C, preferably at 1.5 °C, and strengthen the capacity of countries to respond to the challenge, in a context of sustainable development. In this perspective, the main alternatives found to fossil fuels and the consequent emission of greenhouse gases and climate change are renewable energy sources. These sources can be of various types, such as wind, solar, geothermal, hydroelectric, biomass, waves and tides. Of all renewable energy sources, solar energy has gained relevance over the years, because the energy from the sun is, on a human scale, inexhaustible. However, this type of energy has not yet reached its full potential, due mainly to the price/performance ratio of photovoltaic systems, as photovoltaic cells have low efficiencies (in the order of 15% to 20%).

Therefore, research and development of the use of solar energy is essential in the short, medium and long term, being one of the main sources of "hope" for success in the Paris Agreement, reaching a situation of energy sustainability, such as as can be seen in figure **(1)**, where the evolution of growth in the production of solar energy and wind energy, up to the year 2018, can be seen. In this sense, the motivation of this dissertation is precisely related to the importance, in future terms, of this development and investigation.

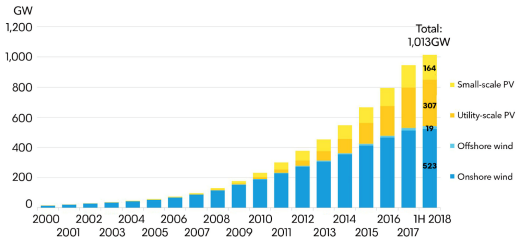

Figure 1: Comparison between the growth of solar and wind energy until 2018.

1.2. Objective

The aim of this work is to develop a structure of photovoltaic panels and thermoelectric generators coupled to power converters, having a maximum power point tracking system. The structure also has a thermoelectric energy conversion system.

1.3. Original Contributions

The original contribution of this work is the development of a system that allows the operation at the maximum power point (MPPT) of the direct transformation of thermal energy (wasted in photovoltaic panels) into electrical energy, from the use of a Thermoelectric Generator, which allows the carrying out of this process as efficiently as possible.

1.4. Document structure

This work is structured into its Theoretical Background (State of the Art), where the physical principles of the Solar Pannel, Thermoelectric Generator, MPPT and Power Converters are explained. However, in this document, Theoretical Background will not be present, focusing on the original contributions and on the system results. As part of the original contributions, the possibility to interconnect an hybrid system containing a Solar Pannel and a Thermoelectric Generator will be shown. As part of the results and conclusion, there will be shown that there is an increase on the efficiency with the same area used in this system.

2. Topology of Photovoltaic Panels and Thermoelectric Generators

2.1. Fresnel Lens

The choice of the type of technology to implement was based on research work on how to increase the temperature of the hot side of thermoelectric modules. This need arises, since the output of the modules tends to be higher at higher temperature differences (keeping the temperature on the cold side, on the hot side, the higher it is, the greater the output power), allowing the same amount of electrical power to be generated with fewer modules.

That said, it is then necessary to reduce the area and concentrate the thermal energy in that same area. In this way, the thermal energy present in the entire area of the panel can be used in a smaller area, where the thermoelectric modules are placed. Note that the solution presented does not allow to directly increase the efficiency of the photovoltaic panel, which is the main disadvantage of this method. Fresnel lenses allow one to reduce the area and keep the radiation, concentrating it in a smaller space. The solution consists in assuming something that, nowadays, is still uncommon, which is the use of a Fresnel lens that takes advantage of the thermal radiation that passes through the photovoltaic panel, allowing this radiation to be concentrated in the area covered by the thermoelectric modules.

It is known that this is possible since the photovoltaic panel radiates energy at its back in the form of infrared radiation. For this purpose, the Fresnel lens in question must be transparent to long-wavelength infrared radiation. The representation of this technology is shown in the figure **(2)**, with the caption as follows: 1 - Fresnel lens; 2 - Sun tracking system; 3 - Thermoelectric module; 4 - Heat extraction system; 5 - Photovoltaic panel; 6 - Solar radiation.

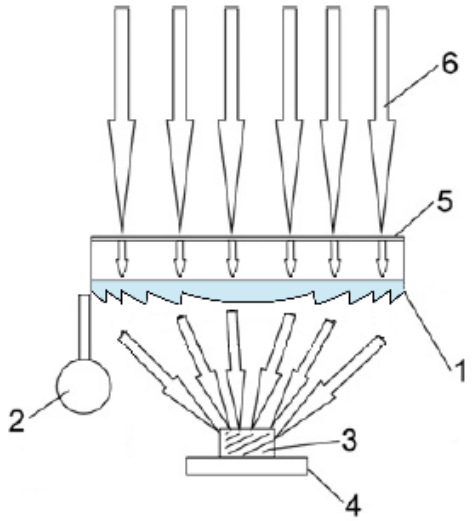

Figure 2: Theoretical representantion of the model to be used in the system (PV-TEG with Fresnel Lens). Adapted from **(1)**.

Note that a photovoltaic panel for the hybrid system must be designed in a special way, providing high thermal conductivity of the substrate and a very polished surface, which is normal for traditional panels: instead of roughness, anti-reflective coating should be used to minimize the reflection **(1)**. Also, the Sun tracking system required for this system can also be simple and inexpensive (although it is not strictly necessary). Thus, we see that TEG with concentrated solar radiation could have a conversion efficiency comparable to that of photovoltaic panels on the market **(1)**.

The cost of thermoelectric modules is slightly higher than that of photovoltaic panels with the same surface area, but taking into account the essential reduction of the TEG area in systems that use radiation concentration, it is concluded that the real cost of generated energy could be acceptable in systems using this principle **(1)**. Knowing that the chosen thermoelectric modules have an efficiency of 14%, it is necessary to determine the diameter of the Fresnel lens to be used in order to obtain 123.6W of electrical power, knowing that this value corresponds to 14% of the incident power. The calculated diameter of the Fresnel lens to be used is 1.10 m. Although it is a very large lens, it will have the advantage of taking advantage of the space already available to produce more energy. Therefore, the efficiency increases, since for the same area it is possible to obtain more energy when implementing this system (increase in energy density).

The calculated balance temperature value is 200 °C, as part of the energy incident on the module flows through it and is dissipated in the heat sink, making the temperature on the hot side of the module to remain constant in this value. Thus, the heat concentrator was used as it allows to concentrate the thermal energy in a smaller area. If a heat concentrator was not used, 66 thermoelectric modules would have to be used. For a temperature of 200°C, only 15 modules are needed, so the solution that includes the concentrator is more economical than simply using them covering the entire back face of the solar panel.

3. Modeling and control of the association of photovoltaic panels and thermoelectric generators

3.1. Photovoltaic Panel and Boost Converter

The first values to be taken into account are provided by the manufacturer, for the maximum power available for the chosen panel (HTM325 345PA-72). This panel was selected due to its high efficiency (17.77% at 345Wp) and good cost/quality ratio. The photovoltaic panel model available in the numerical simulation program used, was used to perform the simulation corresponding to the panel output values. By placing an irradiance and temperature value at the input, the block, through the characteristic values of the panel, simulates the creation of a voltage, current and power at the output.

Note that it was necessary to introduce all the data in this block, thus having a simulation corresponding to the chosen panel. The values to be placed in the block in order to simulate the chosen panel are present in the datasheet and are also represented in the following table,

P_{MP} [W]	V_{MP} [V]	I_{MP} [A]	V_{OC} [V]
345	38.30	9.01	47.00
I_{SC} [A]	μ_{VOC} [mV/°C]	μ_{ISC} [mA/°C]	n_{cells}
9.47	-0.29	0.05	72

Table 1: Electrical and physical parameters of the PV panel.

Using the data in the previous table and the equations that describe the mathematic model of a PV panel, it is possible to arrive, through some manipulation of these same equations, to the values that are presented below, being these the values calculated in the block that simulates the behavior of the photovoltaic panel.

m	R_P [Ω]	R_S [Ω]	I_0 [pA]	I_S [A]
1.48	992.61	0.10	357.52	9.47

Table 2: Calculated values of the parameters for the PV module mathematical model.

Note that, in addition to all the sizing already carried out, in order to produce energy through a photovoltaic system, it is also necessary to ensure that the voltage and current values at the output correspond to an acceptable level, so that it can then pass through the inverter and be injected into the grid. In this way, a boost converter is placed downstream of the photovoltaic panel, so that the voltage level is raised, while the current level is lowered, maintaining power. As known, a boost converter has the capability to raise the voltage up to about 4 or 5 times the value of the input voltage **(2)**. As a voltage value of 400V is intended for the output, since the panel can only produce about 40V, 2 panels will have to be used in series, so its value is close to 80V. Thus, it is already possible to reach the desired voltage value at the output. In figure **(3)** is shown how the system was implemented in the numerical simulation program used, so that one can analyze in more detail what the system includes. To simulate the situation with 2 panels in series, it was necessary to place this information in the corresponding block.

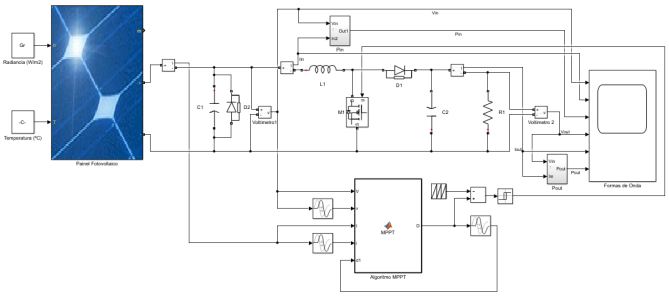

Figure 3: Photovoltaic panel and boost converter with a MPPT algorithm.

Note that it was necessary to place a diode in anti-parallel to the capacitor (bypass) to prevent the possibility of a series connection between 2 or more panels where one of them is shaded, so that the current produced by the others pass through the diode, continuing through the circuit, without damaging them or preventing the shaded panel to limit the system current. It should be noted that, in simulation, the mode of implementation of the system was to parallel the panel and the boost converter with an MPPT algorithm that allows constant analysis and approximation to the maximum power that the panel can produce in certain situations (irradiance and/or temperature conditions).

Regarding the boost converter, it was assumed that an increase was intended to allow the voltage to be set to the desired level (400V) and a proportional decrease in the converter's output current. Thus, calculations were needed so that the filters to be implemented in the converter could be dimensioned. The way in which the calculations were carried out and the results obtained for the values of the filters to be used are shown below. For the input filters, given in the previous figure by L_1 and C_1, where i_E and E are the output current and voltage of the panel and where i_2 and U the values at the output of the boost converter.

Note that a ripple of 5% was assumed for both current and voltage. Thus, and knowing that $T = 1/f$ one has both for the input capacitor and inductor, respectively, **(2)**

$$C_1 = \frac{T\Delta i_2}{8\Delta E} \tag{1}$$

$$L_1 = \frac{UT}{4\Delta i_E} \tag{2}$$

It is also necessary to calculate the capacitor to place at the output of the converter **(2)**

$$C_2 = \frac{I_{UAV}(1-\delta_D)T}{\Delta U} \tag{3}$$

In this way, both the panels and the boost converter to be used, coupled to them, are dimensioned, so that the output values match the intended ones so that they can be placed in parallel with thermoelectric generators and obtain the desired voltage and current values.

3.2. Thermoelectric Generator

As mentioned above, the main objective of this work will be to recover part of the energy of a photovoltaic panel, lost in the form of heat. The element that allows the transformation of heat energy into electricity is the thermoelectric generator. This will be placed in parallel with the solar panel, sharing the output capacitor (C_2), but also having a boost converter downstream of the TEG output. In this work, two Thermoelectric Generators will be used, one for each photovoltaic panel. Thus, it will also be necessary to perform the calculation for the input filters of the boost converter, which are given by C_3 and L_2 as shown below. One has i_E and E as the TEG output current and voltage values and i_2 and U as the values at the boost converter output.

For the capacitor and inductor one has, respectively, **(2)**

$$C_3 = \frac{T\Delta i_2}{8\Delta E} \tag{4}$$

$$L_2 = \frac{UT}{4\Delta i_E} \tag{5}$$

The values of ripple presented are, as in the case of the values considered for the photovoltaic panel, of 5%. The input current and input voltage values will correspond to the datasheet of the chosen thermoelectric generator, taking into account the temperature of the hot side considered ($T_h = 200°C$) and the association in series of 2 TEG (each with 15 thermoelectric modules). In figure **(4)** is represented the scheme of the thermoelectric generator, implemented in the numerical simulation program used, in which the value of the internal resistance is obtained from the equations (7) and (8).

From the figure **(4)**, it is possible to verify that there are several input variables in the system, and of these, the only one that is not known at the outset is the Coefficient of *Seebeck*, being necessary to perform its calculation. The equation that allows one to calculate this value is the following **(4)**

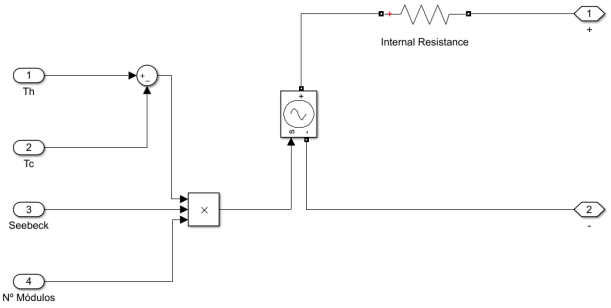

Figure 4: Mathematic model for the Thermoelectric Generator **(3).**

$$C_{Seebeck} = -\frac{\Delta V}{\Delta T} = \frac{V_h - V_c}{T_h - T_c} \tag{6}$$

In the equation for the coefficient of *Seebeck* (6), ΔV is the voltage difference generated between the two conducting metals and ΔT is the temperature difference between the hot and cold sides. The result of calculating the coefficient of *Seebeck* is directly related to another factor. If the semiconductor material is of type n, the carriers are the electrons. In this case ΔV will be positive and in turn the coefficient of *Seebeck* will be negative.

In case the semiconductor material is of type p, which is the case of the material used in the generator chosen for this work, the potential difference will be negative and then the coefficient of *Seebeck* will present a positive value. It is also important to check how the connections of the TEG to the boost converter associated with it are implemented, remembering that its output will be carried out in parallel with the converter associated with the photovoltaic panel, at the capacitor terminals C_2, as shown in figure **(5)**.

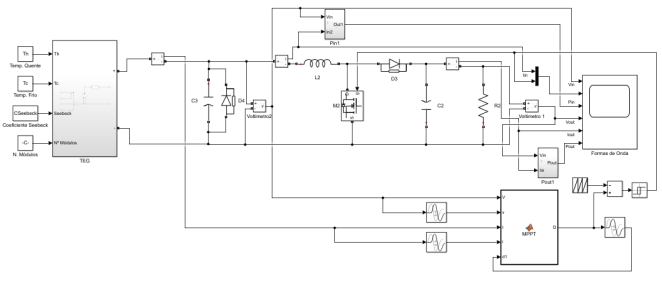

Figure 5: Model for the Thermoelectric Generator with a Boost Converter.

Also in the case of the thermoelectric generator, an MPPT algorithm was used with the same operating principle as that used in the case of the photovoltaic panel.

Finally, as far as the modeling of the system's thermoelectric generator is concerned, the most important factor will be the power it can produce. The power will be influenced by the current value, which is given by **(3)**

$$I_{TEG} = \frac{V_{oc}}{(R_{internal} + R_{load})} \tag{7}$$

Depending on the value of the load resistance and the internal resistance, the power to be drawn from the TEG is given by **(3)**

$$P = V_{oc}^2 \frac{R_{load}}{(R_{internal} + R_{load})^2} \tag{8}$$

Where P is the power generated from the thermoelectric module, being sensitive to load variations. On the other hand, it is directly proportional to the temperature difference, because as the temperature difference increases, the power also increases and, as a result, the maximum power point changes. If a constant load equal to the internal resistance of the thermoelectric module is connected to its terminals, the maximum power point value can be obtained for a given temperature difference. Thus, the ideal value for the internal resistance was calculated, being used both in the internal resistance of the TEG and in the load resistance, in order to validate the model, in the simulations found in chapter 4.

3.3. MPPT Algorithm

So that it is possible for the system to place the maximum possible power at every moment in its output, it is necessary to implement an algorithm that satisfies this need. The algorithm to be used in MPPT will be the algorithm based on the incremental conductance method. Thus, a code will be implemented in the numerical simulation program used, corresponding to a function that will allow putting into practice the flowchart of figure **(6)**.

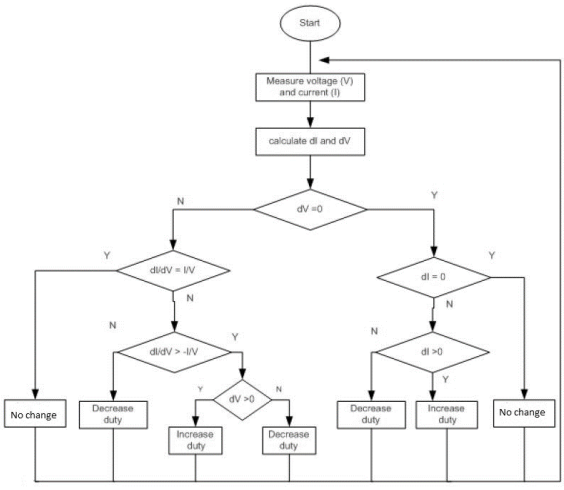

Figure 6: Flowchart for Incremental Conduction Method **(5)**.

Note, however, that the implementation of the code alone is not enough for the algorithm to work, it is still necessary to make the block diagram in represented in figure **(7)**.

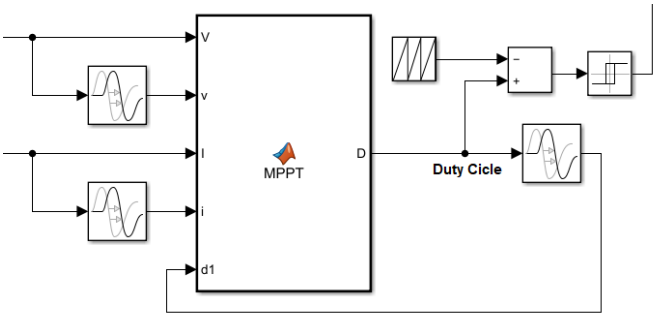

Figure 7: MPPT's Diagram implemented in the system.

It should be noted that the function inputs come from the voltage and current measured at the output of the photovoltaic panel and the thermoelectric generator, while the output of the block diagram represented in the figure will have an input in the gate of the *IGBT*, allowing to carry out a command action on the boost converter. In addition, it is necessary that a delay is performed on both signals (voltage and current), so that a comparison can be made between the value at a given moment and the previous value. At the output of the function, the same applies so that the duty cycle at a certain moment can be compared with the moment that precedes it.

The way the function is introduced in the system is that when the power derivative is positive, the converter command signal takes a minimum value, causing an increase in the input current. Conversely, when the derivative is negative, the command signal goes to its maximum value, which will cause the input current to drop. At the exit, the value is compared with a triangular wave with values between 0 and 1 at the frequency of 20kHz, passing through a hysteresis comparator before entering the gate of the *IGBT*. Finally, it is important to verify how the system reacts with the algorithm of following the maximum power point, represented in figure **(8)**, where the variation of the power for its maximum value assuming a reduction to half of the irradiance.

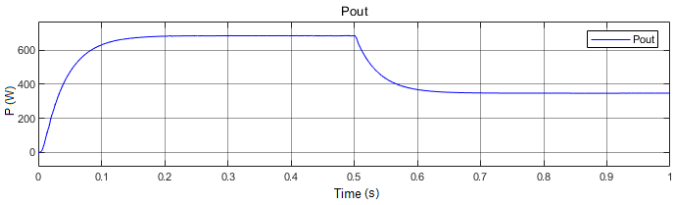

Figure 8: Influence of MPPT on power stabilization when facing a reduction in irradiance.

In the first moments, a smooth rise in the power value is observed, stabilizing without oscillations, having the same behavior when the irradiance decreases at the moment t=0.5 seconds. Figure **(8)** allows validating the MPPT algorithm, since it allows the transition in a smooth way, with a variation in the irradiance value, to the maximum power value under these new conditions.

3.4. Inverter

One now proceeds with an analysis of how the inverter is implemented in the system. Knowing that it is necessary to transform continuous values into alternating ones, so that it can inject energy into the network, it is of great importance that this element works properly. In this way, it is possible to represent V_{pwm} according to the above equation, with this quantity represented in blue in the figure **(9)**.

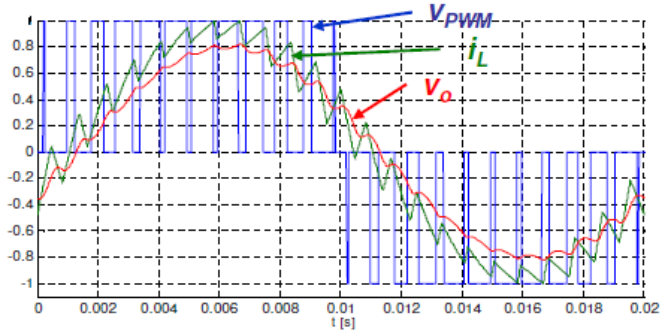

Figure 9: Representation of voltage V_{pwm}, voltage V_0 and current i_L **(2)**.

Now, the representation and analysis of how the inverter was implemented and what it includes, as shown in the figure **(10)**.

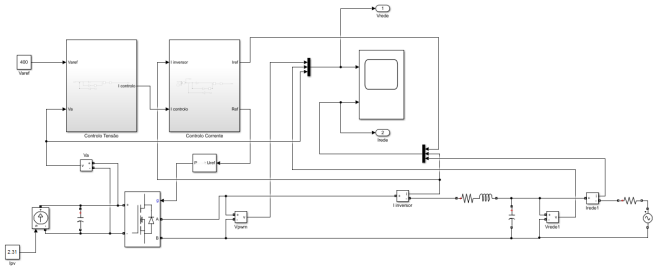

Figure 10: Implementation of the inverter to be used.

The input of the system represented in the figure above corresponds to a controlled current source, as it is the study and dimensioning of the inverter assuming a theoretically ideal situation, before connecting to the rest of the system. The current value used in this source corresponds to the value known to be the output of the step-up converter that will be placed upstream of the inverter in the system. For the proper functioning of the inverter, it is necessary to guarantee the correct functioning of the rest of the system. That said, the values of the inverter's capacitor and output coil were calculated as shown below. The value of the inductor at the inverter output (L_3) is calculated as in a 4-quadrant converter, assuming a ripple of 10% for the nominal value of the current. **(2)**

$$L_3 = \frac{UT}{4\Delta i_{Lmax}} \tag{9}$$

The calculation of the value of the capacitor to be placed at the inverter output (C_4) was performed using the equation shown below, where $\Delta Uemax$ was considered 10% of the nominal value (400V) **(2)**.

$$C_4 = \frac{UT^2}{32L_3\Delta U_{emax}} \tag{10}$$

Note that the capacitor at the input of the inverter (C_5) will be calculated in the context of the voltage control to be carried out on the inverter. In order to obtain the desired values of power to be injected into the network, it is necessary to carry out a control of the values of alternating current and direct voltage, which will be carried out in the inverter and will be analyzed below.

3.4.1. Current Control

The current control is carried out with the purpose of sending a control signal to the input of the PWM Generator at 3 levels, and its output will correspond to the input signal in the gate of the inverter, which is represented by a Rectifying Bridge with 2 arms. In figure **(11)** is represented the input circuit of the inverter.

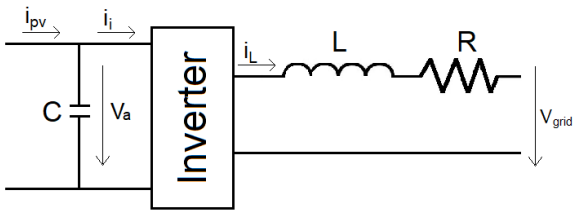

Figure 11: Inverter Input Circuit.

From here, one takes the equation of the dynamics of the current in the inductor, assuming that the resistance is zero, then one has

$$L\frac{dI}{dt} = V_a - V_{grid} \tag{11}$$

Next, in figure **(12)**, the block diagram of the current controller to be implemented is represented, which can be given by a transfer function in which there is a gain G_i and a delay T_d, thus obtaining in the integrator $I = \frac{V_a - V_{grid}}{sL}$.

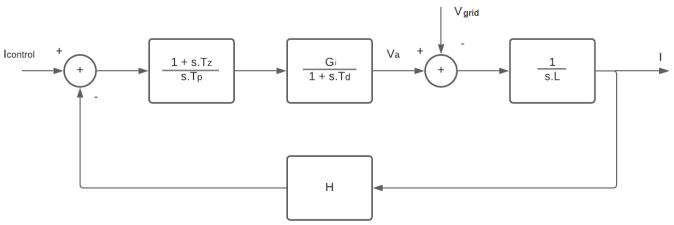

Figure 12: Block diagram for the current controller.

From where the 3rd order Transfer Function can be taken as

$$\frac{I_{inverter}(s)}{I_{control}(s)} = \frac{\frac{1+sT_z}{sT_p}\frac{G_i}{1+sT_d}\frac{1}{sL}H}{\frac{1+sT_z}{sT_p}\frac{G_i}{1+sT_d}\frac{1}{sL}H+1} \tag{12}$$

After some simplifications, and knowing that $H = 1$, one gets

$$\frac{I_{inverter}(s)}{I_{control}(s)} = \frac{1+sT_z}{s^3\frac{T_dT_pL}{G_i}+s^2\frac{T_pL}{G_i}+sT_z+1} \tag{13}$$

Since the transfer function is a 3rd order with a zero, and there is a disturbance (V_{grid}) immediately before the integrator (1/sL), in order to guarantee static zero position error, it is necessary to add a pole at the origin. In order not to increase the excess of poles-zeros, a zero is also added, that is, the compensator will be of the integral proportional (PI) type. To carry out the integral proportional control with total accuracy, it is necessary to calculate the values of K_i (Integral Gain) and K_p (Proportional Gain) to be used in it. To calculate the values of these gains, it is first necessary to calculate the values of the constants T_z, T_d and T_p. Proceeding with the calculations, for T_d a value of $f_c = 20kHz$ is obtained and it is calculated

$$T_d = \frac{\pi}{\omega} = \frac{\pi}{2\pi f_c} \tag{14}$$

It is then possible to use the criteria $b_k^2 = a\ b_{k+1}\ b_{k-1}$, where a represents a degree of freedom of the controller, taking a nonzero value and b_k represents the coefficients. From the transfer function represented in (13) we have that $b_3 = \frac{T_dT_pL}{-G_i}$, $b_2 = \frac{T_pL}{-G_i}$, $b_1 = T_z$ and $b_0 = 1$. Note that, T_p depending on the value of G_i, if it is negative, then T_p will also be, so b_3, b_2, b_1 and b_0 will be positive values. It is then possible to deduce the expressions that will be used to calculate the quantities T_z and T_p, using $a = 2$, where

$$\begin{cases} (\frac{T_pL_3}{G_i})^2 = a\frac{T_pL_3T_d}{G_i}T_z \\ (T_z)^2 = a\frac{T_pL_3}{G_i} \end{cases} \leftrightarrow \begin{cases} T_p = \frac{a^3T_d^2 4G_i}{L_3} \\ T_z = a^2T_d \end{cases} \tag{15}$$

Having this, the values for the gains can finally be obtained as follows

$$K_i = \frac{1}{T_p} \tag{16}$$

$$K_p = \frac{T_z}{T_p} \tag{17}$$

3.4.2. Voltage Control

The voltage on the continuous side will be controlled aiming to make V_a have a value of 400V. From the figure **(11)** it is known that

$$C\frac{dV_a}{dt} = i_{pv} - i_i = i_{pv} - \gamma i_L \tag{18}$$

In average values, γ can be given by G_v. V_{RRMS} is the rms value of the voltage in the network and has the value of 230V and V_a is the value of the voltage at the capacitor at the input of the inverter, having the value of 400V. The value of η was obtained by measurement, when measuring the power at the input of the inverter and at its output, having obtained an efficiency of 97.2%. The capacitor at the inverter input (C_5) will need to be dimensioned so that it can be used in the calculation of the gains present in the voltage control. This capacitor has to be calculated knowing that there is a 100 Hz ripple due to the rectification effect made by the inverter.

Thus, it has the following equation **(2)**

$$C_5 = \frac{I_0}{\omega\Delta V_0} \tag{19}$$

It is necessary to use a constant T_{dv}, which is given by

$$T_{dv} = \frac{\pi}{\omega} = \frac{\pi}{2\times\pi\times f_{grid}} \tag{20}$$

The block diagram for the voltage controller in question is represented as shown in figure **(13)**.

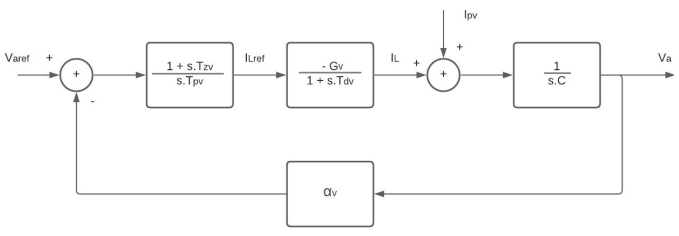

Figure 13: Block diagram for the voltage controller.

From where the 3rd order Transfer Function can be taken from:

$$\frac{V_a(s)}{V_{aref}(s)} = \frac{\frac{1+sT_{zv}}{sT_{pv}}\frac{-G_v}{1+sT_{dv}}\frac{1}{sC}\alpha_v}{\frac{1+sT_{zv}}{sT_{pv}}\frac{-G_v}{1+sT_{dv}}\frac{1}{sC}\alpha_v + 1} \tag{21}$$

After some simplifications, and knowing that $\alpha_v = 1$, one gets

$$\frac{V_a(s)}{V_{aref}(s)} = \frac{1+sT_{zv}}{s^3\frac{T_{dv}T_{pv}C}{-G_v} + s^2\frac{T_{pv}C}{-G_v} + sT_{zv} + 1} \tag{22}$$

Using the criterion $b_k^2 = a\ b_{k+1}\ b_{k-1}$, mentioned before, it is then possible to obtain a way to calculate the constants that will give rise to the calculations of the gains to be used in the controller.

Taking the value of $a = 2$, T_{dv} calculated in (20), $G_v = 0.56$ calculated having in and out values, and C_5 calculated in (19) (which replaces C as it is adapted to the case study), then the constants in question are given by

$$\begin{cases} (\frac{T_{pv}C_5}{-G_v})^2 = -a\frac{T_{pv}C_5T_{dv}}{G_v}T_{zv} \\ (T_{zv})^2 = -a\frac{T_{pv}C_5}{G_v} \end{cases} \leftrightarrow \begin{cases} T_{pv} = \frac{a^3T_{dv}^2(-G_v)}{C_5} \\ T_{zv} = a^2T_{dv} \end{cases} \tag{23}$$

Replacing the values of T_{pv} and T_{zv} in (22) one obtains the closed-chain transfer function as a function of a and T_{dv}

$$\frac{V_a(s)}{V_{aref}(s)} = \frac{1+sa^2T_{zv}}{s^3a^3T_{dv}^3 + s^2a^3T_{dv}^2 + sa^2T_{dv} + 1} \tag{24}$$

Where simplifying, one finally obtains,

$$\frac{V_a(s)}{V_{aref}(s)} = \frac{1+sa^2T_{zv}}{(1+saT_{dv})(s^2a^2T_{dv}^2 + s(a^2-a)T_{dv} + 1)} \tag{25}$$

Having this, one now performs the calculations for the gains and the values are obtained through these equations,

$$K_{iv} = \frac{1}{T_{pv}} \tag{26}$$

$$K_{pv} = \frac{T_{zv}}{T_{pv}} \tag{27}$$

As a way to show all the results obtained through the equations present in this chapter, the table 3 is presented, where all the values calculated for the filters and for the controll parameters are shown.

R_{Load}	173.1 Ω	T_p	706.0 µs
C_1	0.141 µF	T_z	100.0 µs
C_2	3.240 µF	T_d	25.00 µs
C_3	0.037 µF	T_{pv}	-1.082 s
C_4	0.036 µF	T_{zv}	0.040 s
C_5	368.0 µF	T_{dv}	0.010 s
L_1	1.109 mH	k_i	1420
L_2	42.59 mH	k_p	0.142
L_3	21.63 mH	k_{iv}	-0.924
$C_{Seebeck}$	0.036	k_{pv}	-0.030

Table 3: Results for the filters and parameters calculated.

4. Results of Simulations and Discussion

The *Boost* output capacitor terminals were interconnected to the rectifier bridge input terminals, which allows the conversion of quantities with a direct value into an alternate value. In this way, the voltage at the output of the step-up converter directly influences the power values that the inverter places on the grid. Taking this into account, three different simulations in Matlab were performed to validate the model. First, the system was simulated under normal conditions assuming full power delivery to the grid. Secondly, the simulation of the system was carried out, assuming that all the generated energy would be delivered to the electrical grid, varying the irradiance by half of its original value.

Thirdly, a simulation of the system was carried out in which it was assumed that there was a load to be fed, in order to simulate a house, with a variation in irradiance by half and then by double. As mentioned before, 2 solar panels had to be placed in series, since the output voltage of a single panel is too low compared to the network voltage, and there is no capacity on the part of the elevator converter to carry out this conversion in the voltage value (about 10 times higher).

The results obtained are shown in figure **(14)**, where the output quantities of the indicated systems can be observed, from 0.4 seconds, since the transient in the simulation results is neglected. Thus, the images present in this subchapter are all starting in 0.4 seconds because from this time forward it is possible to observe only the steady state, which is what really matters in terms of analysis.

The current that goes to the inverter never takes constant values, it is an impulsive current because the inverter has semiconductors that either set the correct value of the current, or set the value to zero, since the inverter has 3 levels. Thus, when the output voltage is zero, the inverter does not put current in the output. Regarding the first simulation, the voltage and current waveforms to be injected into the network are represented in figure **(15)**.

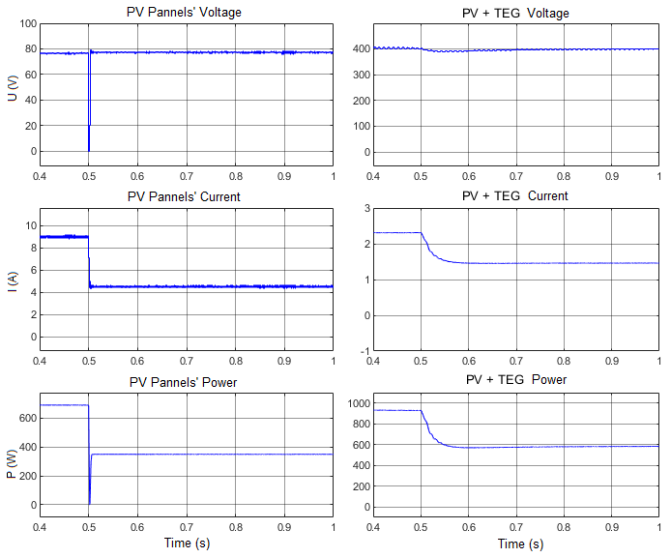

Figure 14: Waveforms at the output of the photovoltaic panel and the PV-TEG system.

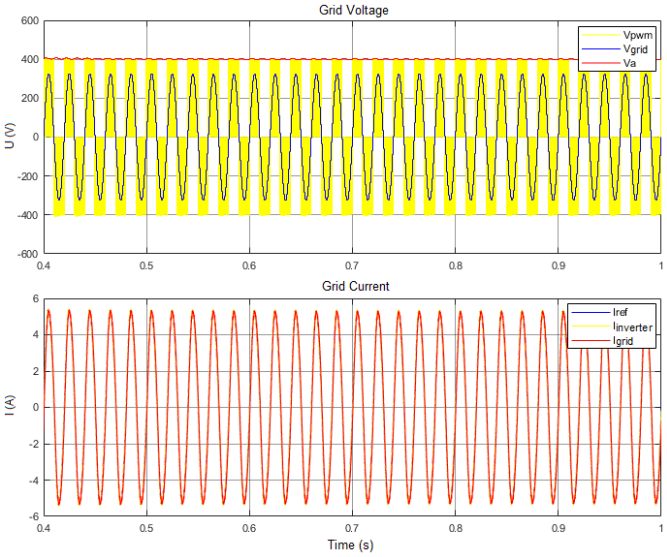

Figure 15: Wave forms generated by the system.

In terms of inverter efficiency, it is possible to confirm the value present in subsection 3.4.2 of 97.2% from the figure **(15)** since it is known that the power of input to the inverter is 924.6W (two 345W photovoltaic panels and two thermoelectric generators that add 117.3W each) and the output power of 897W (effective voltage value of 230V and effective current value of 3.9A) in case of irradiance $G = 1000W/m^2$.

The results of the second simulation, in which the system was only connected to the power grid and the irradiance was reduced to half, are shown in figure **(16)**, where one can see this happening in more detail.

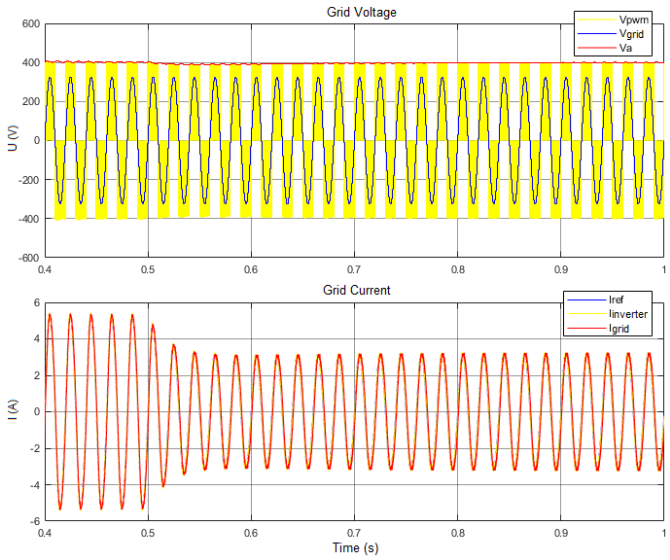

Figure 16: Waveforms at the exit of the system, with a decrease in irradiance.

Regarding the third simulation, the test was carried out on whether the system could fulfill the purpose of supplying a domestic load, having placed the load resistance in parallel with the network. Thus, the following waveforms were observed for the voltage and current in the system, represented in the figure **(17)**.

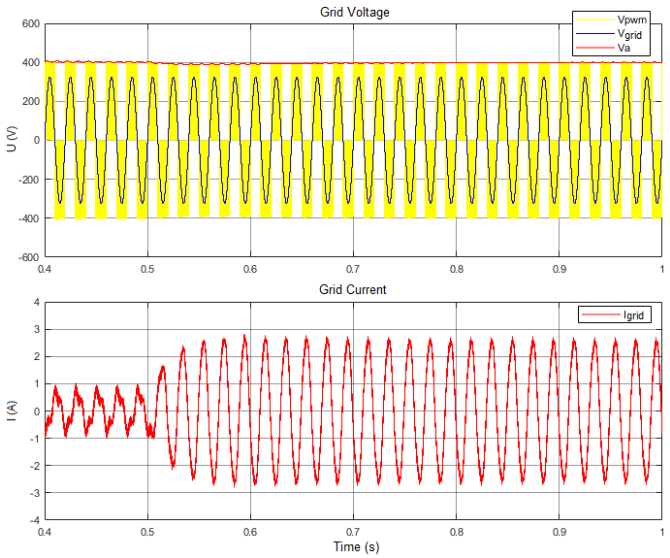

Figure 17: Waveforms at the output of the system when feeding a load when irradiance decreases.

It is observed that up to 0.5 seconds, the current has a very low value (since the panel is under maximum irradiance conditions) and is thus only feeding domestic consumption, leaving little power to flow to the network. After 0.5 seconds, the irradiance decreases to half, making the system need to use the network to supply the load (it

can be seen that current and voltage are in anti-phase at this moment, comparing I_{grid} with V_{grid} from 0.5 seconds to 1 second). Finally, in order to validate the simulation, it was necessary to test the inverse situation, and at 0.5 seconds the irradiance is no longer half and becomes maximum, simulating a hypothetical cloud no longer shading the panel. The result is shown in figure **(18)**.

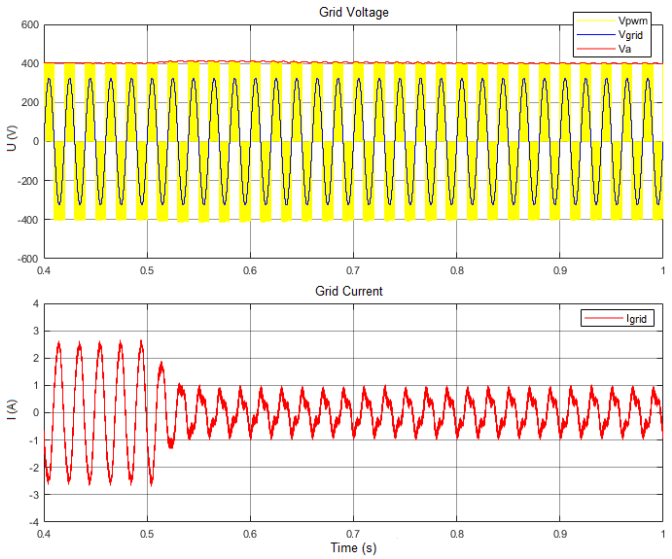

Figure 18: Waveforms at the output of the system when feeding a load when irradiance increases.

The distortions that occur in the current waveform when it has a value close to zero, are related to the fact that the controller used is linear. One of the features of this controller is to control the voltage better than the current. Thus, when it is close to zero, there are harmonics to be introduced from the network to the circuit (in order to complete the little power that is needed to satisfy the load, when we are faced with the situation of irradiance $G = 1000W/m^2$). Furthermore, the voltage controller, by not having a constant DC value, will also contribute harmonics to the distortion of the current waveform. Finally, it should be noted that when the controller wants a quick response to variations, and by having this speed, loses quality regarding the distortion of the waveforms.

5. Conclusions and Future Work

5.1. Conclusions

In the study of the system, several solutions were presented in order to obtain a higher energy efficiency in a PV-TEG system than in a system that was only composed of photovoltaic panels. It was found that it was possible, in fact, to obtain an increase in efficiency while keeping the system relatively economical. In terms of system modeling, the necessary calculations and dimensions were carried out so that the system is in balance and could be interconnected, working as one in the production and more efficient use of solar and thermal energy. Thus, taking all these issues into account, controllers were implemented in the inverter, so that the system could be viable, either to make an interconnection to the electrical grid or to supply a domestic load, maintaining the required voltage levels network and home equipment.

It should be noted that there were slight differences in the theoretical values calculated with the values obtained in the simulations, namely with regard to the thermoelectric generator, in which a generated power of about 5% less than expected was obtained. Even so, it was possible to validate the model and find the ideal solution to implement the system. The most important conclusion to be drawn from this dissertation is that it is in fact possible to increase the efficiency of a photovoltaic panel, through the use of thermoelectric modules connected in parallel to it, making use of its heat. In numerical terms, the efficiency increased from 17.8% (690W) for the chosen panels, to about 23.8% (924.6W) after implementing the parallel with the TEGs. These efficiency values are taking into account the area of 2 panels and irradiance under ideal conditions.

5.2. Future Work

As a future approach to the present problem in this work, it should be noted that this remains an underdeveloped area in scientific terms at a global level, therefore it is interesting from the point of view of technological development to analyze what was considered and the solutions presented. Thus, it is recommended the physical implementation of the system, performing tests and analyzing results under real conditions, checking the possibilities presented.

References

[1] Chávez-Urbiola, E. A., Vorobiev, Y. V., Bulat, L.P.: *Solar hybrid systems with thermoelectric generators*. 2011.

[2] Silva, J. F. A.: *Electrónica Industrial: Semicondutores e Conversores de Potência*. 2013 Fundação Calouste Gulbenkian.

[3] Mamur, H., Çoban, Y.: *Detailed modeling of a thermoelectric generator for maximum power point tracking*. 2019.

[4] Antonio, R. C., Eugenio, R. G., José, C. A.: *Development and automation of a thermoelectric characterization system*. 2018.

[5] Anowar, M. H. and Roy, P.: *A Modified Incremental Conductance Based Photovoltaic MPPT Charge Controller*. 2019 International Conference on Electrical, Computer and Communication Engineering (ECCE), February 2019.

[6] Paterakis, F., Marouchos, C. C., Darwish, M.: *Comparison of a PWM Inverter and a Multilevel Inverter using the Switching Function Analysis for Harmonic Content and Efficiency*. 2017.